

Rheological Properties and Chemical Bonding of Asphalt Modified with Nanosilica

Hui Yao, Ph.D.¹; Zhanping You, Ph.D., P.E., M.ASCE²; Liang Li, Ph.D.³; Chee Huei Lee, Ph.D.⁴; David Wingard, Ph.D., M.ASCE⁵; Yoke Khin Yap⁶; Xianming Shi, Ph.D., P.E., M.ASCE⁷; and Shu Wei Goh, Ph.D.⁸

Abstract: The objective of this study is to evaluate the rheological properties and chemical bonding of nano-modified asphalt binders blended with nanosilica. In this study, the nanosilica was added to the control asphalt at contents of 4% and 6% based on the weight of asphalt binders. Superpave binder and mixture tests were utilized in this study to estimate the characteristics of the nano-modified asphalt binder and mixture. The rotational viscosity (RV), dynamic shear rheometer (DSR), bending beam rheometer (BBR), Fourier transform infrared spectroscopy (FTIR), scanning electron microscopy (SEM), asphalt pavement analyzer (APA), dynamic modulus (DM) and flow number (FN) tests were used to analyze rheological properties and chemical bonding changes of the nano-modified asphalt binder and the performance of the nano-modified asphalt mixture. In addition, the performance of nano-modified asphalt after rolling thin-film oven (RTFO) short-term and pressure-aging vessel (PAV) long-term aging was assessed as well. The dissipated work per load cycle for the asphalt binder was used to evaluate the rheological properties of the nano-modified asphalt binder. Based on the binder test results, it was found that the additional nanosilica in the control asphalt binder slightly decreased the viscosity of the control asphalt binder, maintained low dissipated work per load cycle, held a similar low-temperature performance to the control asphalt, and had a positive effect on antioxidation. From the mixture test results, the dynamic modulus and flow number of nano-modified asphalt mixtures improved, and the rutting susceptibility of nano-modified asphalt mixtures was reduced compared to the control asphalt mixture. In general, the findings from this study show that the antiaging property and rutting and fatigue cracking performance of nanosilica modified asphalt binders are enhanced, and the addition of nanosilica in the control asphalt mixture significantly improves the dynamic modulus, flow number, and rutting resistance of asphalt mixtures. DOI: 10.1061/(ASCE)MT.1943-5533.0000690. © 2013 American Society of Civil Engineers.

CE Database subject headings: Rheology; Asphalts; Nanotechnology; Mixtures; Bonding; Chemical properties.

Author keywords: Rheological; Asphalt; Nanomaterial; Nano-modified asphalt; Fourier transform infrared spectroscopy (FTIR); Nanosilica; Scanning electron microscopy (SEM); Asphalt mixture.

¹Research Assistant, Dept. of Civil and Environmental Engineering, Michigan Technological Univ., 1400 Townsend Dr., Houghton, MI 49931-1295. E-mail: huiyao@mtu.edu

²Associate Professor, Dept. of Civil and Environmental Engineering, Michigan Technological Univ., 1400 Townsend Dr., Houghton, MI 49931-1295 (corresponding author). E-mail: zyou@mtu.edu

³Professor, School of Civil Engineering and Architecture, Central South Univ., Changsha, Hunan, 410075, China. E-mail: liliang_csu@126.com

⁴Postdoctoral Research Associate, Dept. of Physics, Michigan Technological Univ., 1400 Townsend Dr., Houghton, MI 49931-1295. E-mail: chlee@mtu.edu

⁵Research Assistant Professor, Dept. of Civil Engineering, Clemson Univ., Clemson, SC 29634. E-mail: Wingar2@clemson.edu

⁶Professor, Department of Physics, Michigan Technological Univ., 1400 Townsend Dr., Houghton, MI 49931-1295. E-mail: ykyap@mtu.edu

⁷Associate Research Professor, Civil Engineering, Western Transportation Institute, Montana State Univ., Bozeman, MT 59717-4250. E-mail: Xianming_s@coe.montana.edu

⁸Research Assistant, Dept. of Civil and Environmental Engineering, Michigan Technological Univ., 1400 Townsend Dr., Houghton, MI 49931-1295. E-mail: sgoh@mtu.edu

Note. This manuscript was submitted on December 13, 2011; approved on September 18, 2012; published online on September 22, 2012. Discussion period open until April 1, 2014; separate discussions must be submitted for individual papers. This paper is part of the *Journal of Materials in Civil Engineering*, Vol. 25, No. 11, November 1, 2013. © ASCE, ISSN 0899-1561/2013/11-1619-1630/\$25.00.

Introduction

Asphalt has a complicated chemical composition, which exhibits both viscous and elastic properties that heavily depend on both time and temperature (Yildirim 2007; Peters et al. 2010). Researchers and engineers have been trying to use various kinds of modifiers to modify and improve the asphalt materials' performance, including styrene butadiene styrene (SBS) (Cortizo et al. 2004; Al-Hadidy and Yi-qiu 2011), styrene-butadiene-rubber (SBR) (Zhang et al. 2005; Zhang et al. 2009), ethylene glycidyl acrylate (EGA) terpolymer (Yildirim 2007), crumb rubber (Shen et al. 2009; Xiao et al. 2009), organo-montmorillonite (Yu et al. 2007a; Sun et al. 2008; Yu et al. 2009), waste tire rubber (Goulias 2001; Cao 2007), and fibers and waste fibers (Putman and Amirkhani 2004; Anurag et al. 2009; Peters et al. 2010). SBR has been widely utilized as a binder modifier, usually as a latex disperser. According to the reports of the U.S. Federal Aviation Administration, SBR-modified asphalt binder can optimize the properties of asphalt concrete pavement and seal coats. It can also improve the low-temperature, elastic recovery, and adhesive and cohesive performance of the pavements. When the SBR is mixed with asphalt, it is rapidly and uniformly melted and forms the reinforced network structure (Zhang et al. 2005; Yildirim 2007; Zhang and Yu 2010). In addition, EGA terpolymer can react with asphalt as a modifier. Based on the research conducted by Yildirim et al., EGA

terpolymer can improve the moisture damage potential of asphalt mixtures, and it has a higher fracture temperature in combination with granite (Yildirim 2007). Some researchers have used the diatomite and cellulose to modify the asphalt binder, and the results show that its high-temperature and low-temperature performance can be improved (Peters et al. 2010; Cong et al. 2012). Previous research also shows that the organo-montmorillonite has positive effects on the aging performance of asphalt. It can be well dispersed into the asphalt and polymer matrix. The addition of organo-montmorillonite can lead to enormous reinforcements of thermal and mechanical properties of asphalt binders (Zhang et al. 2005; Yu et al. 2007a, b; Yu et al. 2009; Zhang et al. 2009).

Styrene butadiene styrene (SBS) is most widely used as a modifier around the world. Many researchers tried to investigate the microstructure and pavement performance of SBS modified asphalt binder (Cortizo et al. 2004; Al-Hadidy and Yi-qiu 2011; Zhang et al. 2011). The results show that SBS modified asphalt significantly improves the fatigue cracking and low-temperature performance (Yildirim 2007; Larsen et al. 2009). Research has used waste materials as asphalt additives, such as waste fibers, waste tire rubber, waste plastic, and tall oil pitch (Hansen et al. 2000; Lindberg et al. 2008; Arabani et al. 2010).

Nanotechnology is a promising and creative technique in the material industry, and nanomaterials have been widely applied to the various fields of the entire world. The carbon nano-fiber was used for the asphalt binder modification. The mixing procedure, viscoelastic, and fatigue characteristics of control and carbon nanofibers (CNFs) modified asphalt binder were investigated in the research. From the viscosity and dynamic shear rheometer (DSR) test results, the viscoelastic response and rutting resistance of CNFs modified asphalt binder were improved, as well as the fatigue life (Khattak et al. 2011, 2012). Raw SWNT (single-wall nanotube) materials were adopted to modify the asphalt binder. The tests including viscosity and DSR were conducted to evaluate the high-temperature performance of the modified asphalt binder. The performance grade temperature of the modified asphalt binder increased and the low thermal sensitivity of the modified asphalt binder was observed. In addition, the elastic component of complex shear modulus in the modified asphalt binder was higher than the control asphalt binder (Shiman et al. 2011). The various contents (0.5, 1.0, and 1.5% by weight of the base asphalt binder) of carbon nanoparticles were used to modify the control asphalt binder (five binder sources: PG 64-22, PG 64-16, and PG 52-28). The rheological characteristics of modified asphalt binders after the rolling thin-film oven (RTFO) processing were studied, including the failure temperature, performance grade, and creep recovery. The results of these tests indicate the improvement of complex shear modulus, failure temperature, and elastic modulus in the modified asphalt binders. Additionally, the binder source dose significantly influences the rheological properties of modified asphalt binders (Xiao et al. 2011). Recently, the nonmodified nanoclay (NMN) and polymer modified nanoclay (PMN) were used as the additives to modify the asphalt binder. The rotational viscosity, DSR, and SEM were employed to test the performance of modified asphalt binders. The test results show that the additional nonmodified nanoclay increased the viscosity and complex shear modulus of the modified asphalt binder, and the addition of polymer modified nanoclay slightly decreases the viscosity and complex shear modulus of the modified asphalt binder. The rutting resistance performance of NMN and PMN modified asphalt binder and mixture may be improved through the binder microstructure changing (Yao et al. 2012). In addition, the nanoclay also has recently been used for asphalt modification. With the addition of nanoclay in the asphalt binder, the high-temperature of modified asphalt binders improves (You et al. 2011). The asphalt

mixtures modified by polysiloxane-modified montmorillonite and/or carbon microfiber can decrease the moisture susceptibility of asphalt mixture (Shi et al. 2012).

Nanosilica material (NS) has been applied to medicine, drug delivery, and engineering. The merits of nanosilica (chemical formula SiO_2) material are the low cost of production and high performance features (Lazzara and Milioto 2010). Nanosilica is a relatively new inorganic material that is used due to its potentially beneficial properties (e.g., huge surface area, strong adsorption, good dispersal ability, high chemical purity, and excellent stability). Nanosilica has been used as an additive, catalyst carrier, rubber strength agent, plastic filler, and as a graphite viscosity agent, among other uses in various industries. Due to these potentially beneficial properties, nanosilica has the potential to be used as an asphalt modifier for improving asphalt performance.

In this study, the nanosilica was used to modify the control asphalt binder. It was added into the control asphalt binder at concentrations of 4% and 6% by weight of the base asphalt binder. Asphalt binder and mixture tests such as the rotational viscosity (RV), dynamic shear rheometer (DSR), bending beam rheometer (BBR), asphalt pavement analyzer (APA), dynamic modulus (DM) and flow number (FN) tests were conducted to evaluate the performance, and microstructure examinations of the nano-modified asphalt binder (NMA) were carried out using scanning electron microscopy (SEM) and Fourier transform infrared spectroscopy (FTIR). Details of the tests and discussions of the results obtained from the testing are found in the following sections.

Experimental Procedures

1. Rotational viscosity (RV): The degree of asphalt binder fluidity is generally estimated by the viscosity. The purpose of rotational viscosity is to check the pumping and handling ability of asphalt during storage, mixing and compaction. It can be used for nonmodified and modified asphalt binders [ASTM-D2196 (ASTM 2010b); Al-Khateeb and Al-Akhras 2011]. In addition, three samples will be used in the test.
2. Dynamic shear rheometer (DSR): The DSR test is to measure the properties of asphalt binders at intermediate to high temperatures. It shows the asphalt binder's resistance to permanent deformation and fatigue cracking [ASTM-D7405 (ASTM 2010a)]. Since the asphalt binder is viscoelastic, the phase angle is between 0° and 90° . A phase angle of 0° represents an elastic solid and a phase angle of 90° is a viscous liquid. Permanent deformation resistance is measured on the unaged and RTFO-aged asphalt binders and the fatigue cracking is measured on the PAV-aged asphalt binder [13°C is the lowest temperature in the DSR machine used; 21.3°C is the Michigan fatigue effective temperature which was conducted in related research work (You et al. 2009); 32°C is the middle temperature of 21.3°C and 39.2°C ; 39.2°C is the Michigan rutting effective temperature which was conducted in related research work (You et al. 2009); 46°C , 64°C , 70°C are PG grade temperatures; and 54.4°C is the E^* testing temperature].
3. Bending beam rheometer (BBR): The creep stiffness of asphalt binders versus loading time is determined by the BBR test. The test results show the relationship between the low temperature and asphalt binders, and indicate the stress relaxation when constant loading (0.98 N) is applied in the asphalt beam [ASTM-D6648 (ASTM 2008); Liu et al. 2010]. The test temperature is -24°C in this study.
4. Fourier transform infrared spectroscopy (FTIR): According to the different infrared absorbance of chemical bonding in

the FTIR machine, the FTIR test is used for the functional characteristic analysis of asphalt binders (Xu and Huang 2010a, b). FTIR spectra are recorded by Jasco IRT 3000 FTIR spectrometer. For the measurement in the transmission mode, a silicon substrate with 350 μm thickness was used and the thin asphalt binder sample was spread on the silicon substrate.

- Scanning electron microscope (SEM): In order to observe the surface morphology and analyze microstructure characteristics of nanosilica, an Hitachi S-4700 field emission scanning electron microscope (FE-SEM) was used in the study (Probst et al. 2007). The Hitachi S-4700 FE-SEM is a cold field emission, high-resolution, scanning electron microscope. Images of control and nano-modified asphalt binders were taken by using a Hitachi SU6600 FE-SEM equipped with a cryogenic stage. The binder samples were flash frozen using liquid nitrogen and then placed in the SEM chamber at -26°C under a pressure of 30 Pa. The cryogenic stage was used in order to reduce changes in the binder structure due to heating by the 20-kV electron beam used during examination.
- Dynamic modulus (E^*): According to Report 465 of National Cooperative Highway Research Program (NCHRP) (Witczak et al. 2002), three candidate simple performance tests (SPTs) were recommended to evaluate the overall performance of asphalt mixtures, including the dynamic modulus, flow time and flow number tests. The report also concluded that these laboratory tests have good correlation with the occurrence of pavement distress in the field pavements and prediction for rutting and fatigue cracking. The dynamic modulus test monitors the relationship between the stress and strain under a continuous sinusoidal loading for linear viscoelastic materials, and the relationship is defined as dynamic modulus ($|E^*|$). It is mathematically calculated using the maximum (peak) dynamic stress (σ_0) divided by the peak recoverable axial strain (ε_0) (Witczak et al. 2002; Witczak 2007):

$$|E^*| = \frac{\sigma_0}{\varepsilon_0}, \quad \phi = \frac{t_i}{t_p} \times 360 \quad (1)$$

where E^* = dynamic modulus; ϕ = phase angle; σ_0 = applied stress amplitude; and ε_0 = measured strain amplitude with linear variable displacement transducers (LVDTs); t_i = time lag between stress and strain cycles; and t_p = time for a stress cycle.

In this study, according to American Association of State Highway and Transportation Officials (AASHTO) TP62, an IPC universal testing machine (UTM-100) was used in this research. The test was conducted under the temperatures of -10°C , 4°C , 21.3°C , and 39.2°C and at the frequencies of 25, 10, 5, 1, 0.5, and 0.1 Hz.

- Asphalt pavement analyzer (APA) rutting: Laboratory wheel-tracking devices are used to simulate and evaluate the mixture stripping and rutting potential. These accelerated tests require less time and effort to measure the rutting performance of asphalt mixtures and predict the field performance (Goh et al. 2011). In this study, according to AASHTO TP63-03, asphalt pavement analyzer (APA) was used to test the rutting depth of the asphalt mixture. The test was carried out under the condition of 58°C and 8,000 loading cycles.
- Flow number: The repeated load flow number (F_n) test, a dynamic creep test, is used to measure the specimen's permanent strain under a haversine type of loading. The cumulative permanent strain curve can be separated into three areas: primary, secondary, and tertiary. Flow number, a cycle number, indicates the beginning of tertiary flow. Flow number, also a simple performance test, can be correlated with rutting

potential (Witczak et al. 2002, 2007). From the literature review (Goh and You 2009; Goh et al. 2011), in this study, a new stepwise method was used to determine the flow number. Based on the average annual air temperature of Michigan, an average of T_{eff} rutting of 45°C was obtained from the Michigan Department of Transportation (MDOT) report. The temperature was also selected in the test. The air void of asphalt mixture samples was $7\% \pm 1\%$, and the standard samples are 100 mm in diameter and 150 mm in height.

Experimental Materials

Nanosilica

In this research, the nanosilica was purchased from MTI Corporation (U.S.A.) without further treatment, featuring a bulk density of 0.063 g/cm^3 , maximum size of about 30 nm, and surface area of about $440 \text{ m}^2/\text{g}$ (He and Shi 2008). In most cases, the Si atom centers at the tetrahedron with four oxygen atoms surrounding the Si atom. Quartz crystalline form of silica SiO_2 is common and all four oxygen atoms are shared with others (Iler 1979; Greenwood and Earnshaw 1998; Wiberg et al. 2001). In addition, the nanosilica is presented in the form of quartz and cubic polymorph (Fig. 1). From the FE-SEM images of nanosilica and nanosilica modified asphalt binders (Fig. 1), some agglomerations can be seen in the nanosilica material and asphalt binder, but for the most part the material is well dispersed in the asphalt binder. The agglomerations can be attributed to the Ostwald ripening phenomenon (Mrotzek and Nembach 2008; An et al. 2012) and van der Waals attraction force. Ostwald ripening is a phenomenon in which small crystals or solution particles dissolve and redeposit onto larger crystals or solution particles. If some of the nanosilica particles agglomerated, they would be in the order of micrometers instead of nanometers. However, some of nanosilica would stay at the nanometer size, and exhibit a large surface area. Potentially, the chemical reactions would be accelerated. From the spectra analysis, the Si-O (Si) asymmetric stretching bands located at $1,085 \text{ cm}^{-1}$ and the asymmetric vibration of Si-O (H) is near 975 cm^{-1} . The results of FTIR spectra (Fig. 2) are consistent with this.

Control Asphalt and Modified Asphalt Binders

The control asphalt binder PG 58-34 was obtained from a pavement project in Gladstone, Michigan. It was noted that the control PG 58-34 asphalt had been modified with acrylonitrile butadiene styrene (ABS) to improve the compatibility between polymer and asphalt (Cortizo et al. 2004) and thermal degradation (Dong et al. 2001). This control binder was modified with nanosilica in the lab. The nanosilica material was added into the control asphalt binder at concentrations of 4% and 6% by weight of the control asphalt binder, and mixed in the high shear rate machine (Silverson L4RT-A Laboratory Mixer). It was observed that once the nanosilica had dispersed and melted in the control asphalt binder, the surface of the asphalt binder had a few floating bubbles. During the mixing, the binder samples were kept at 130°C and blended using a shear rate of 4,000 revolutions per minute (rpm) for two hours.

Results and Discussion

Rotational Viscosity Test Results of Asphalt Binders

Fig. 3 shows that, with the addition of nanosilica material in the PG 58-34 control asphalt binder, the viscosity of nanosilica modified

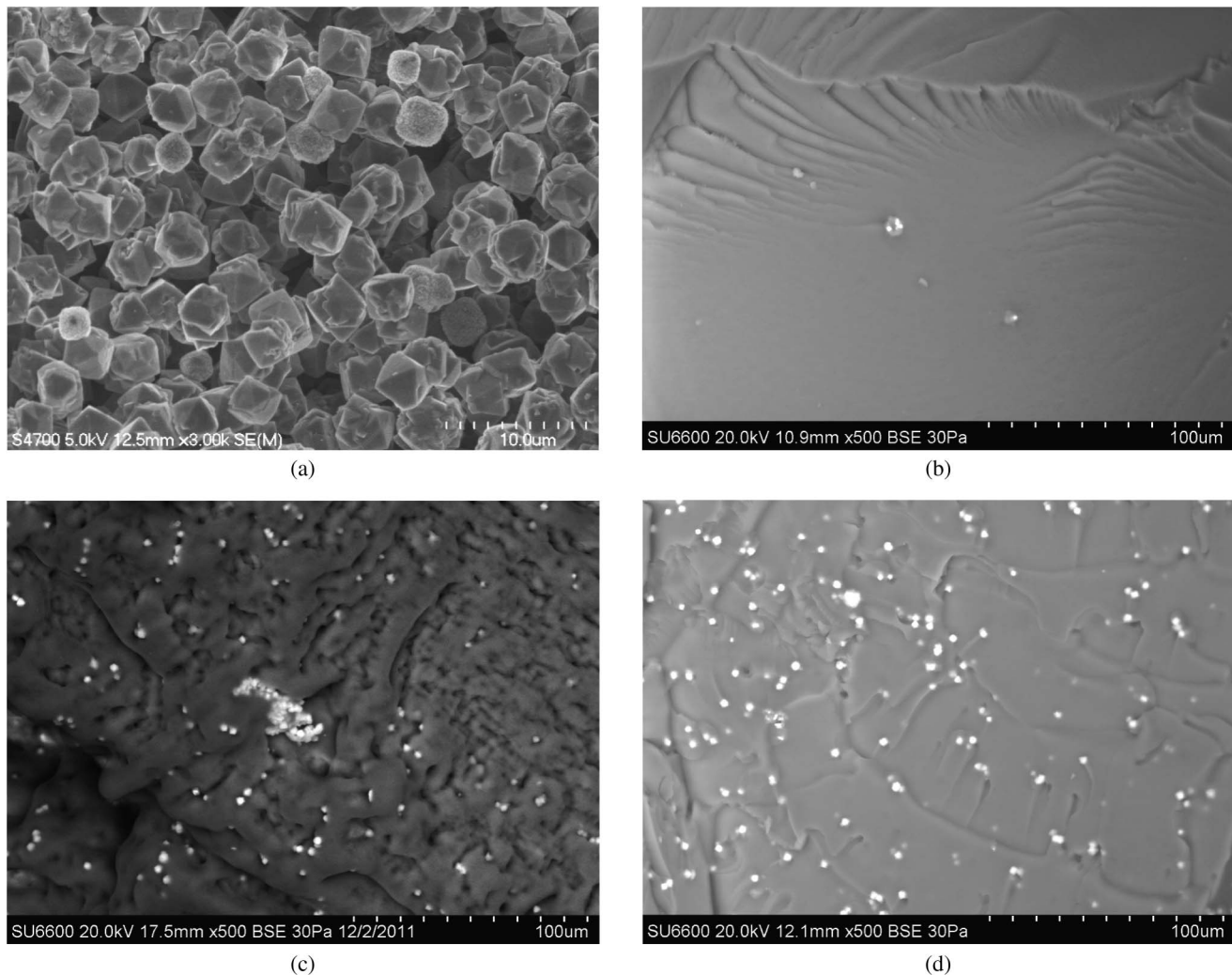


Fig. 1. FE-SEM microstructure images of nanosilica, control and nanosilica modified asphalt; (a) SEM image of nanosilica at 3,000× magnification; (b) SEM image of control asphalt binder at 500× magnification; (c) SEM image of 4% nanosilica modified asphalt binder at 500× magnification; (d) SEM image of 6% nanosilica modified asphalt binder at 500x magnification

asphalt binder decreases by an average of 4%. Meanwhile, it is evident that viscosity values at the Superpave standard specification temperature of 135°C were passed, and nanosilica modified asphalt had viscosity values lower than the maximum limit of 3 Pa. In addition, the mixing process of nanosilica modified asphalt binder suggest that those chemical reactions and physical dispersion are likely to happen, and a new network structure might be formed (demonstrated later). Due to the temperature resistance of nanosilica, the viscosity of modified asphalt binder decreases slightly. Furthermore, nanosilica holds the potential to strengthen the control asphalt binder and to improve the recovery ability when stress is applied.

Complex Shear Modulus ($|G^*|$) Test Results of Asphalt Binders

Dynamic shear rheometer (DSR) is used to characterize the viscous and elastic behavior of asphalt binders at high temperatures. From the parallel plate tests, the average complex shear modulus ($|G^*|$) and phase angle (δ) of asphalt binders can be determined (Goh et al. 2007; You et al. 2011). For rutting dissipated work, the calculation equation (Bahia and Anderson 1995; Brown 2009) is shown in

Eq. (2), and for fatigue cracking dissipated work, the calculation equation (Bahia and Anderson 1995; Brown 2009) is shown in Eq. (3):

$$\text{Rutting: } Wc = \pi\sigma_0^2 \left(\frac{1}{G^*/\sin \delta} \right) \quad (\text{stress-controlled}) \quad (2)$$

$$\text{Fatigue cracking: } Wc = \varepsilon_0^2 (G^* \sin \delta) \quad (\text{strain-controlled}) \quad (3)$$

where Wc = work dissipated per load cycle; σ = stress applied during load cycle; ε = strain during load cycle; G^* = complex shear modulus; and δ = phase angle

In addition, with each cycle, when the load is applied, the work from each loading is applied into the pavement. A portion of the work is reflected as elastic rebound. However, the remaining work is transferred into permanent damage, such as rutting, fatigue cracking and crack propagation. Therefore, the low work dissipated per loading cycle indicates the good performance of resistance to rutting and fatigue cracking (Asphalt Institute 2003). However, in this research, the strain controlled model of test was adopted to compute the rutting and fatigue cracking dissipated work of the asphalt binder. Thus, the high dissipated work per load cycle of

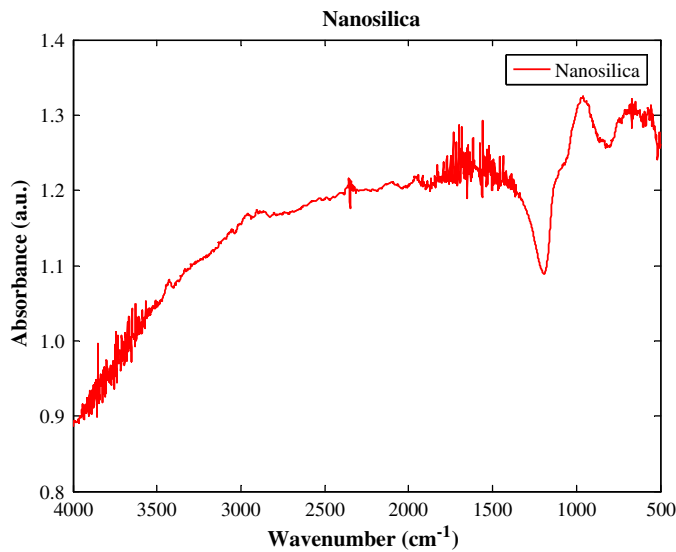


Fig. 2. FTIR spectra analysis of nanosilica

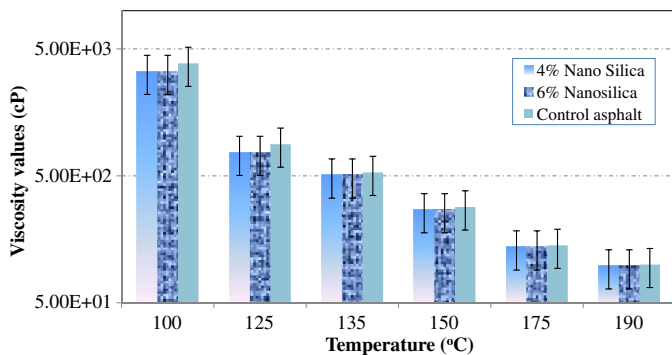


Fig. 3. Viscosity values of control and nanosilica modified asphalt binder

the asphalt binder is better for the rutting resistance performance, and the low dissipated work per load cycle in the asphalt binder is better for the fatigue cracking prevention performance.

Dynamic Shear Rheometer (DSR) Results of Original Asphalt Binders

Fig. 4 demonstrates that the control asphalt binder has higher complex shear modulus than that of nanosilica modified asphalt binder. With the addition of nanosilica into the control asphalt, the complex shear modulus decreases by an average of 20%. Meanwhile, considering the high rigidity of nanosilica, with the addition of nanosilica in the control asphalt binder, it can be obtained from lower complex shear modulus results and the phenomena during the binder mixing that the chemical reactions and physical dispersion happened and a new structure of asphalt binder was formed. Note that the potential reactions may include those between the surface $-OH$ groups of nanosilica and certain chemical groups in the asphalt binder. Because of the presence of silane coupling agent (ABS) (Kim et al. 2003; Chotirat et al. 2007), the hydroxyl groups on the inorganic nanoparticles convert to various organic functional groups (Sugimoto 2000; Ding et al. 2009). That reacting hydroxyl with silane coupling agents leads nanosilica from hydrophilic surfaces to hydrophobic surfaces (Sugimoto 2000; Ding et al.

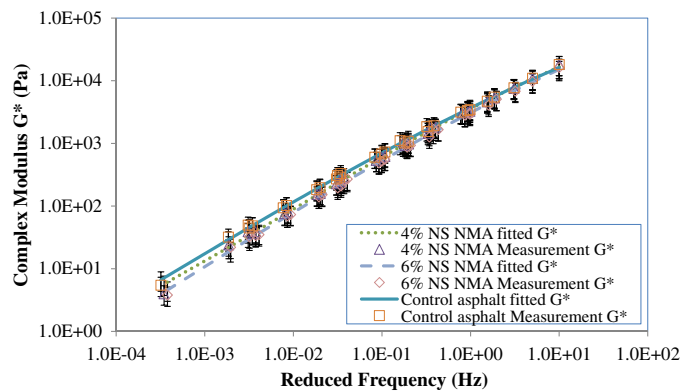


Fig. 4. Complex shear modulus (G^*) master curves of nanosilica modified asphalt binder and control asphalt binder (with standard error bars)

2009). That microstructure causes the lower complex shear modulus and resists more fatigue cracking at high temperatures. Additionally, the dissipated work per load cycle of rutting was calculated and shown in Fig. 5.

Fig. 5 shows the amounts of dissipated work per loading cycle of nanosilica modified asphalt binder are lower than the control asphalt binder. In other words, the low work of nanosilica modified asphalt binders may be transferred into the forms of distresses when the loading is applied. The addition of nanosilica into the control asphalt binder may improve the recovery ability of asphalt binders. In addition, due to the modification of nanosilica, modified asphalt binder may absorb more work and transfer more work, and the mechanical performance and fatigue cracking prevention of asphalt binders may be enhanced. Therefore, the nanosilica modified asphalt binder potentially may have better rutting resistance performance relative to the control asphalt binder.

Dynamic Shear Rheometer (DSR) Results of Asphalt Binders after RTFO Aging

From Fig. 6, the complex shear modulus master curves of nanosilica modified asphalt binder and control asphalt binder are represented. It is noticed that with the addition of nanosilica in the control asphalt binder, the complex shear modulus of nano-modified asphalt binders decreases slightly after RTFO aging process. With the addition of 4% nanosilica in the control asphalt binder, the complex shear modulus decreases by an average of 8%

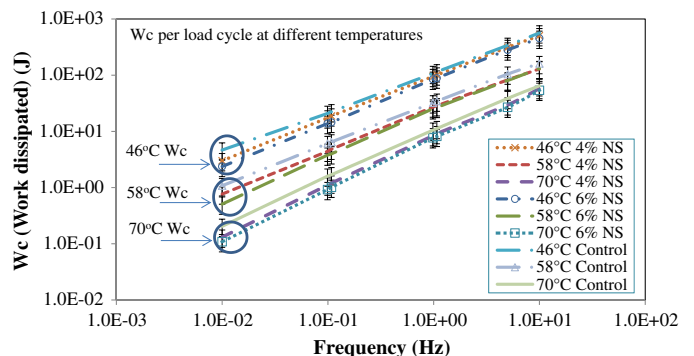


Fig. 5. Work dissipated per load cycle of nanosilica modified asphalt binder and control asphalt binder (rutting influence, with standard error bars)

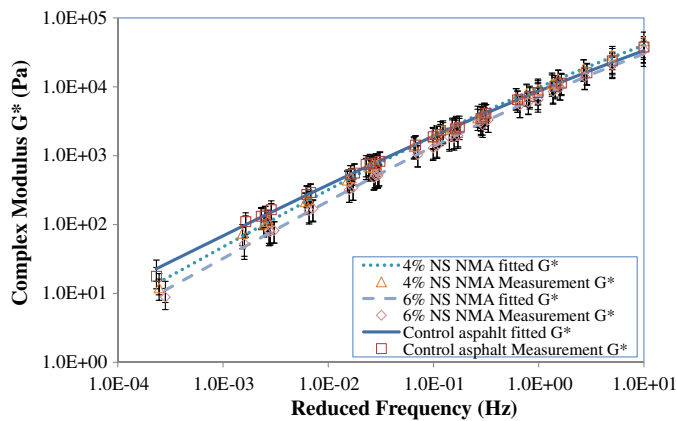


Fig. 6. Complex shear modulus ($|G^*|$) master curves of control and nanosilica modified asphalt binder after RTFO aging process (with standard error bars)

while 6% nanosilica modified asphalt binder decreases by an average of 12%, the modulus values are so close in the nanosilica modified asphalt binder. During the mixing and heating process, nanosilica may react chemically with the control asphalt binder, and the more stable structure is formed from the FTIR test results below. As such, the modified asphalt can become more viscous and feature low complex shear modulus after RTFO aging.

The dissipated work per load cycle of rutting influence was calculated and shown in Fig. 7. Fig. 7 shows that the dissipated work of nanosilica modified asphalt binder is lower than the control asphalt binder after RTFO aging process. In addition, from the work standpoints and microstructure images, nanosilica is melted homogeneously in the control asphalt binder and improves the recovery ability of the binder. When the loading is applied, the remaining work in the nanosilica modified asphalt is less and the less work converts to the distress of asphalt binder. Therefore, with the addition of nanosilica into the control asphalt binder, the performance of resistance to rutting in the nano-modified asphalt mixture can be improved.

Dynamic Shear Rheometer (DSR) Results of Asphalt Binders after PAV Aging

Fig. 8 shows that with the addition of nanosilica in the control asphalt binder, the complex shear modulus of nano-modified asphalt

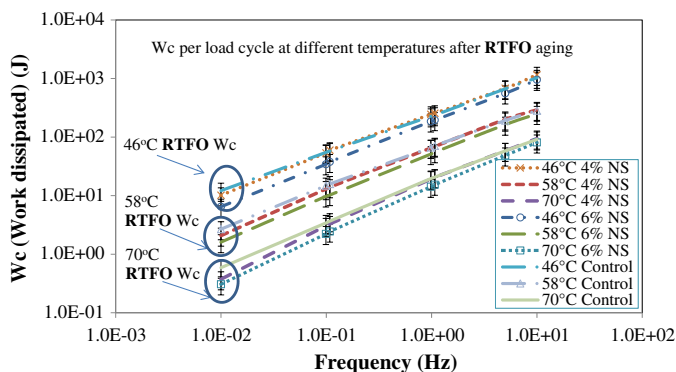


Fig. 7. Work dissipated per load cycle of control and nanosilica modified asphalt binder after RTFO aging process (rutting influence, with standard error bars)

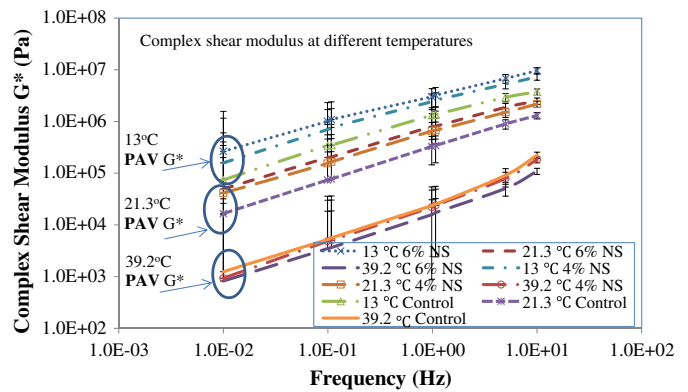


Fig. 8. Complex shear modulus G^* of control and nanosilica modified asphalt binder after PAV aging process (with standard error bars)

binders decreases slightly at the high temperatures after PAV aging process. However, the complex shear modulus increases significantly at around 21.3°C and 13°C. At high temperatures, the nanosilica modified asphalt binder can absorb and transfer more work, as well as preventing the fatigue cracking. Meanwhile, it shows more recovery performance during the loading cycles. At around 13°C, the nanosilica modified asphalt binder may become stiffer than the control asphalt binder, but that does not influence the low temperature performance.

The nanosilica modified asphalt binder at 39.2°C (a relatively high temperature) showed outstanding performance. The potential explanation is provided as follows. Inorganic nanoparticles have demonstrated great potential to mitigate the aging of polymeric materials (Odegard et al. 2005; Balazs et al. 2006), which is typically initiated by thermal scissions of carbon-carbon (C-C) bonds associated with a transfer of hydrogen radical at the site of scission. Once mixed, the nanoparticles and polymer chains can strongly interact through the branching effect, nucleation effect, size effect, and surface effect, markedly slowing down the polymer's aging process and increasing the decomposition temperature. Nanomaterials with low surface potential work can migrate to the surface of composites at elevated temperatures and serve as a heating barrier to protect host polymers in the cases such as organomodified-MMT/rubber (Sun et al. 2008) and nano-silica (SiO_2)/rubber system (Peng et al. 2007; Chen et al. 2008). Asphalt binder is mostly a polymeric system and the benefits of nanosilica to the aging resistance of asphalt are thus anticipated.

One recent study reported that when added at 4wt% nano- SiO_2 was homogeneously distributed throughout the natural rubber matrix in a form of a spherical nanocluster with an average size of 80 nm, which significantly enhanced the rubber's thermal resistance. The authors however also reported the possible side effects of nanosilica addition to rubber especially its low temperature properties and heat accumulation of the nanocomposite, which may explain the poor effects of nanosilica modified asphalt at 13°C (Chen et al. 2008). The nanosilica modified asphalt binder at 13°C temperature starts to appear to be brittle in the test, and the BBR test results of nanosilica modified asphalt demonstrate the coincidence with 13°C modulus result. In addition, the fatigue cracking dissipated work of nanosilica modified asphalt binder and control asphalt binder is calculated and shown in Fig. 9.

From Fig. 9, it can be seen that nanosilica modified asphalt binder has lower dissipated work than the control asphalt binder at 39.2°C. However, at 21.3°C and 13°C, the control asphalt binder almost has the same dissipated work as nanosilica modified asphalt

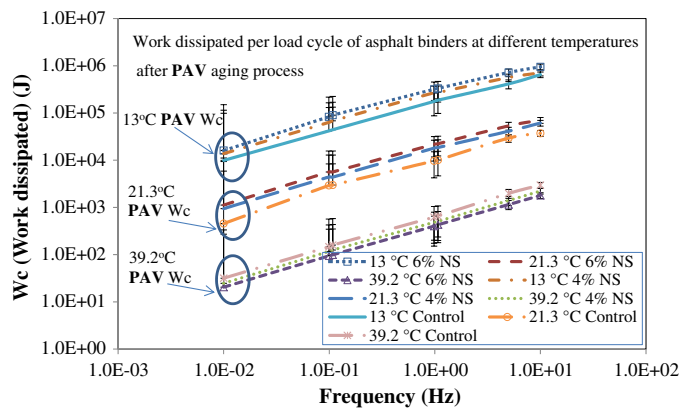


Fig. 9. Work dissipated per load cycle of control and nanosilica modified asphalt binder after PAV aging process (fatigue cracking influence, with standard error bars)

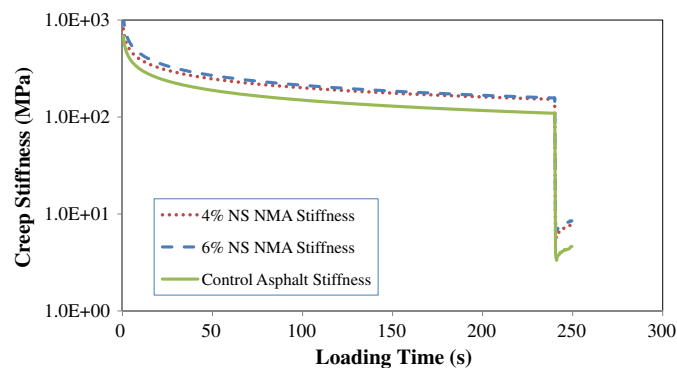


Fig. 10. Creep stiffness of control and nanosilica modified asphalt binder in BBR test

binders. The dissipated work of nanosilica modified asphalt binder is higher than the control asphalt binder. After the PAV aging process, the fatigue cracking performance becomes more important. From the work perspective, the nanosilica can delay the aging effect of modified asphalt binders and hold more prevention from the fatigue cracking distress.

BBR Test Results of Asphalt Binders

Fig. 10 shows the creep stiffness of nano-modified asphalt binder and control asphalt binder in the bending beam rheometer test. It demonstrates the ability of stress relaxation and low temperature performance in the nano-modified asphalt binder. The control asphalt binder has higher deflections and lower creep stiffness than the nanosilica modified asphalt binders. These results reflect the work perspective of modified asphalt binder at 13°C after the PAV aging process. In addition, from Table 1, the stiffness of control and nano-modified asphalt binders at the 60-second loading

time are lower than 300 MPa and all m-values at the 60-second mark are higher than 0.300. All passed the Superpave specification requirements. The low-temperature grade of the nanosilica-modified asphalt binder is the same as the control asphalt. So, the additional nanosilica in the control asphalt does slightly affect the low-temperature performance; also it is not enough to make a low-temperature grade change.

SEM Images Analysis

The SEM images of nanosilica modified asphalt are helpful to understand the microstructure change of modified asphalt, as well as the physical dispersion of nanosilica particles. As shown in Fig. 1, the microstructure of nanosilica modified asphalt binder was changed significantly compared to the control asphalt binder. The SEM images of nanosilica modified asphalt binder present the well-dispersed nanosilica particles in the asphalt matrix. Due to the agglomeration of nanosilica, the surface of nanosilica group reacts with the asphalt binder, and the size of nanosilica group becomes smaller. The new structure of nanosilica modified asphalt binder is formed, and the nanosilica group, white particles in asphalt matrix, is glued uniformly with the asphalt binder. The nanosilica dispersion in the asphalt binder may be helpful for the modulus improvement of nanosilica modified asphalt mixture. In addition, from the FTIR (Figs. 11–13) of control and nanosilica modified asphalt binder, the ratio of stretching OH group in the asphalt, which is centered around $3,594\text{ cm}^{-1}$, and $3,735\text{ cm}^{-1}$, is increased. It also proves that nanosilica is physically dispersed in the asphalt. From the SEM and FTIR examinations it can be seen that the new constituents from reactions and dispersions have high melting and boiling points, and may improve the temperature resistance of modified asphalt binders.

FTIR Test Results of Asphalt Binders

In this study, the FTIR test was employed to evaluate the chemical bonding changes of control and nanosilica modified asphalt binder, and the results are shown in Figs. 11–13. In the Figures, the strong peaks around $2,850\text{ cm}^{-1}$ and $2,920\text{ cm}^{-1}$ is typical C-H stretching vibrations in aliphatic chains (Larsen et al. 2009). The peak at around 966 cm^{-1} is attributed to bending C-H trans-disubstituted $-\text{CH}=\text{CH}-$ of butadiene block (ethylene band). The band at around $1,030\text{ cm}^{-1}$ is assigned to stretching sulfoxide. The aliphatic branched band (bending C-H of CH_3) and aliphatic index band (bending C-H of $-(\text{CH}_2)_n-$) are observed at $1,376\text{ cm}^{-1}$ and $1,460\text{ cm}^{-1}$ respectively. The $1,600\text{ cm}^{-1}$ and $1,690\text{ cm}^{-1}$ bands correspond to the aromatic band (stretching C=C aromatic) and carbonyl band, (stretching C=O conjugated) respectively (Ouyang et al. 2006; Larsen et al. 2009; Zhang et al. 2011).

In Figs. 11–13, it is apparent that the FTIR Figure trends of control and nanosilica modified asphalt binder is different between 975 cm^{-1} and $1,400\text{ cm}^{-1}$. That proves the microstructure of nanosilica modified asphalt binder is changed relative to the control asphalt binder, and it corresponds with the previous guess. In addition, the unaged, RTFO-aged and PAV-aged FTIR figures

Table 1. m-Values and Stiffness of Control Asphalt Binder and Nanosilica Modified Asphalt Binder at 60 Seconds in the BBR Test

Asphalt binder type	Temperature (°C)	Time (s)	Deflection (mm)	Measured stiffness (MPa)	m-value	Remarks
Control asphalt binder	-24	60.0	0.445	178	0.317	Pass the specification
4% nanosilica-modified asphalt binder	-24	60.0	0.341	234	0.306	Pass the specification
6% nanosilica-modified asphalt binder	-24	60.0	0.314	252	0.301	Pass the specification

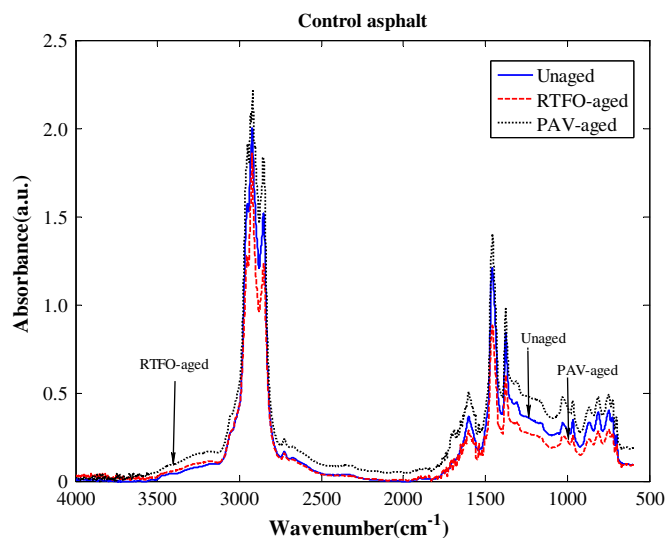


Fig. 11. FTIR spectra analysis of control asphalt binder

trends of control and nanosilica modified asphalt binder are similar. In order to estimate the chemical bonding changes and avoid the thickness effect of the asphalt sample films, the peaks area ratio of bands were used and calculated from Eqs. (4)–(9) (Ouyang et al. 2006; Larsen et al. 2009; Zhang et al. 2011). The bands ratio changes results are shown in Table 2:

$$I_{\text{CH}=\text{CH}} = \frac{\text{Area of the ethylene band centered around } 966 \text{ cm}^{-1}}{\sum \text{Area of the spectral bands between } 2000 \text{ cm}^{-1} \text{ and } 600 \text{ cm}^{-1}} \quad (4)$$

$$I_{\text{S}=\text{O}} = \frac{\text{Area of the sulfoxide band centered around } 1030 \text{ cm}^{-1}}{\sum \text{Area of the spectral bands between } 2000 \text{ cm}^{-1} \text{ and } 600 \text{ cm}^{-1}} \quad (5)$$

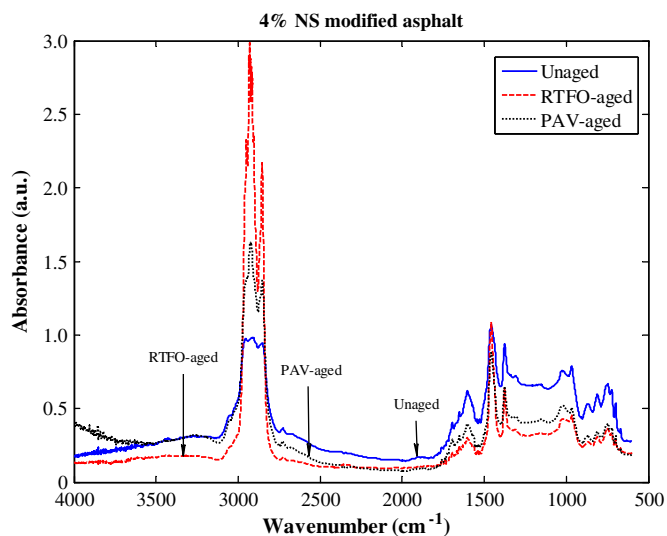


Fig. 12. FTIR spectra analysis of 4% nanosilica modified asphalt binder

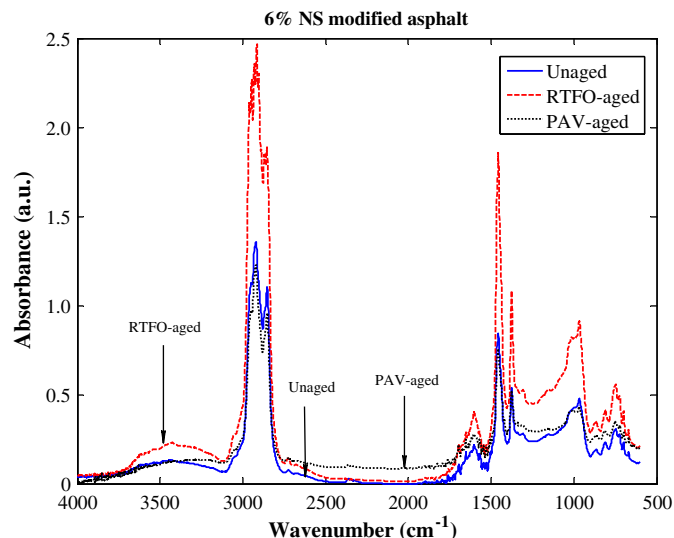


Fig. 13. FTIR spectra analysis of 6% nanosilica modified asphalt binder

$$I_{\text{C-H of CH}_3} = \frac{\text{Area of the aliphatic branched band centered around } 1376 \text{ cm}^{-1}}{\sum \text{Area of the spectral bands between } 2000 \text{ cm}^{-1} \text{ and } 600 \text{ cm}^{-1}} \quad (6)$$

$$I_{\text{C-H of }-(\text{CH}_2)_n-} = \frac{\text{Area of the aliphatic index band centered around } 1460 \text{ cm}^{-1}}{\sum \text{Area of the spectral bands between } 2000 \text{ cm}^{-1} \text{ and } 600 \text{ cm}^{-1}} \quad (7)$$

$$I_{\text{C}=\text{C}} = \frac{\text{Area of the aromatic band centered around } 1600 \text{ cm}^{-1}}{\sum \text{Area of the spectral bands between } 2000 \text{ cm}^{-1} \text{ and } 600 \text{ cm}^{-1}} \quad (8)$$

$$I_{\text{C}=\text{O}} = \frac{\text{Area of the carbonyl band centered around } 1690 \text{ cm}^{-1}}{\sum \text{Area of the spectral bands between } 2000 \text{ cm}^{-1} \text{ and } 600 \text{ cm}^{-1}} \quad (9)$$

Table 2 demonstrates the ratio changes of bands in the control and nanosilica modified asphalt binder. Based on the literature review (Leontaritis and Mansoori 1988; Mansoori 1997; Cortizo et al. 2004; Ouyang et al. 2006; Larsen et al. 2009; Xu and Huang 2010a; Zhang et al. 2011), the carbonyl (C=O) and aromatic indexes (C=C) will be increased after the RTFO and PAV aging. However, sulfoxide index (S=O) in the asphalt mostly increases after the RTFO aging process and probably decreases after the PAV aging process. Therefore, the sulfoxide index is not suitable for the aging index, and carbonyl index is chosen as an aging index. From the Table 2, the carbonyl index of nanosilica modified asphalt binder increased after the PAV aging process, however, it decreased slightly after the RTFO aging process relative to the unaged binder. That means that with the addition of nanosilica into the control asphalt, the aging process of asphalt binders may be weakened and delayed. The asphaltenes, aliphatic, and resins are the most important compounds in the asphalt, and asphaltenes are hydrogenated

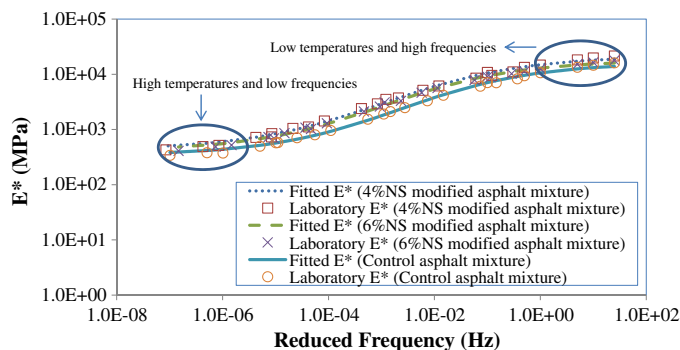
Table 2. Ratio Changes of Bands before or after the RTFO and PAV Aging Process

Samples	CH=CH	S=O	C=O	C=C	C-H of $-(CH_2)_n-$	C-H of CH_3
	966 cm^{-1}	1,030 cm^{-1}	1,690 cm^{-1}	1,600 cm^{-1}	1,460 cm^{-1}	1,376 cm^{-1}
Unaged Samples						
4% NS NMA	0.0574245	0.065691	0.0079028	0.0323977	0.109517	0.0363381
6% NS NMA	0.0837	0.0894472	0.0056894	0.0264402	0.136381	0.0441487
Control asphalt	0.0436405	0.0523013	0.0047064	0.0357135	0.164433	0.0554052
RTFO Samples						
4% NS NMA	0.0595707	0.0674036	0.0071389	0.0280833	0.123831	0.0389095
6% NS NMA	0.0812086	0.0909166	0.0053566	0.0263309	0.142902	0.044338
Control asphalt	0.0430544	0.0537932	0.005529	0.035892	0.156063	0.0526021
PAV Samples						
4% NS NMA	0.0579449	0.0704871	0.0090425	0.0327154	0.106815	0.035585
6% NS NMA	0.0628599	0.0691674	0.0077374	0.028495	0.105464	0.0358896
Control asphalt	0.0436232	0.0543756	0.0080897	0.0358174	0.138736	0.0472945

into the polycyclic aromatic or hydroaromatic hydrocarbons (carbon atoms form rings). Therefore, the aromatic amount increased in the asphalt binder after the RTFO and PAV aging processes. In addition, the aliphatic compounds are opposite to the aromatic compounds in the organic chemistry. The carbon atoms in the aliphatic are arranged in a linear chain. When the asphalt is heated, the aliphatic compounds soften first and make the asphalt temperature sensitive. After the RTFO and PAV aging, the asphalt binder becomes stiff and the aliphatic molecules in the asphalt binder will decrease. Because of the ABS modification in the control asphalt (Dong et al. 2001; Cortizo et al. 2004), the ethylene index is noticed in the FTIR test images. The ethylene index (CH=CH) decreased in the asphalt binder after the RTFO and PAV aging processes, and it shows that poly-butadiene part in the asphalt underwent the degradation during the RTFO and PAV aging processes. In summary, the nanosilica material is a good modifier in inhibiting oxidizing reactions in the asphalt binder.

Dynamic Modulus Test Results of Asphalt Mixtures

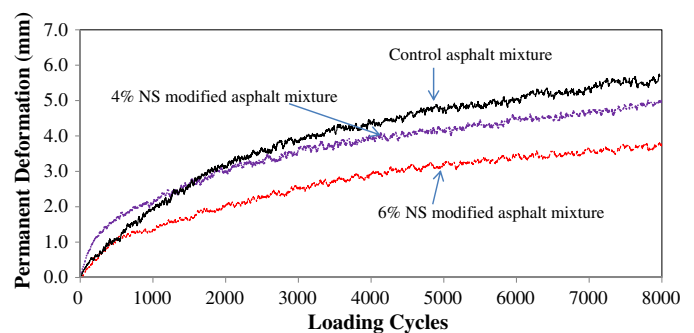
Fig. 14 shows the dynamic modulus results of control and nanosilica modified asphalt mixtures. The dynamic modulus of nanosilica modified asphalt mixture is higher than the control asphalt mixture. The additional nanosilica in the asphalt mixture improves the modulus of asphalt mixture by an average of 30%. The results indicate that the nanosilica modified asphalt mixture has more possibilities to resist the permanent deformation compared to the control asphalt mixture. The dynamic modulus of 6% nanosilica modified asphalt mixture is slightly higher than the 4% nanosilica

**Fig. 14.** Dynamic modulus results of control and nanosilica modified asphalt mixtures

modified asphalt mixture at the high temperatures, and lower than the 4% nanosilica modified asphalt mixture at the low temperatures. These results imply the 6% nanosilica modified asphalt mixture is softer than 4% nanosilica modified asphalt mixture at low temperatures and stiffer at high temperatures. Compared to 4% nanosilica modified asphalt mixture, 6% nanosilica modified asphalt mixture has better high-temperature and low-temperature performance. It is possible that the more nanosilica is added in the control asphalt, the higher dynamic modulus of nanosilica modified asphalt mixture is shown. The microstructure of asphalt binders partly determines the macro-performance of asphalt mixture. In the SEM images (Fig. 1) of nanosilica modified asphalt binder, the structure of asphalt binders strengthens the bonding connections between the aggregates and asphalt binder compared to the control asphalt binder. Meanwhile, the multilayer structures of the nanosilica-modified asphalt binder are probably similar to the calcium silica hydrate (CSH) and calcium hydroxide (CH) structures of concretes with nanosilica. These changes in the asphalt binder and mixture cause the dynamic modulus improvement of nanosilica modified asphalt mixture.

APA Rutting Test Results of Asphalt Mixtures

Fig. 15 displays the APA rut depths of control and nanosilica modified asphalt mixtures. As shown in the figure, the nanosilica modified asphalt mixture has the lower depths than the control asphalt mixture, and the rut depths of 6% nanosilica modified asphalt mixture is also lower than the 4% nanosilica modified asphalt mixture. APA rutting test is a kind of simulative tests for the pavement performance evaluation at high temperatures, and the test results have

**Fig. 15.** APA rutting results of control and nanosilica modified asphalt mixtures

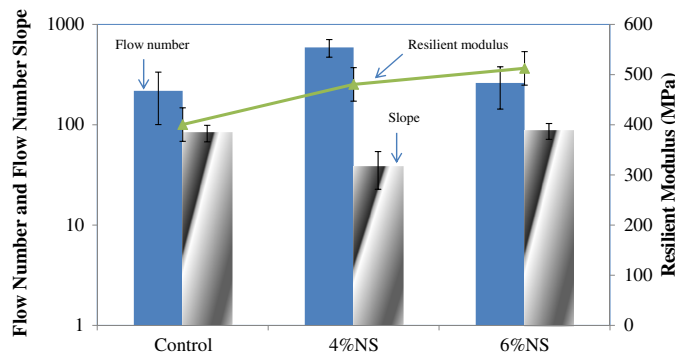


Fig. 16. Flow number results of control and nanosilica modified asphalt mixtures

good correlation with the field data. It is noted that the rutting susceptibility of asphalt mixture is reduced significantly with the additional nanosilica in the control asphalt. As shown in the SEM images of nanosilica modified asphalt binder (Fig. 1), the structure of modified asphalt binder are good for strengthening the coating property of asphalt binders compared to the control asphalt binder. As stated above, the reacting between the asphalt binder and nanosilica makes the nanosilica from the hydrophilic surfaces to hydrophobic surfaces. Due to the microstructure changings of nanosilica modified asphalt binder, the bonding property between the aggregates and binder may be enhanced, and the dense framework structure of nanosilica modified asphalt mixture may be formed. These transformations of nanosilica modified asphalt binder also are critical to increase the possibility to resist the rutting of asphalt pavement at high temperatures. The antistripping property of asphalt mixture also increases with the addition of nanosilica in the control asphalt mixture. The APA results of control and nanosilica modified asphalt mixtures are coincident with the prediction from dynamic modulus data.

Flow Number Test Results of Asphalt Mixtures

Fig. 16 demonstrates the flow number results of control and nanosilica modified asphalt mixtures. The flow number value of control asphalt mixture is lower than the nanosilica modified asphalt mixture. With the addition of nanosilica into the control asphalt mixture, the flow number of nanosilica modified asphalt mixture increases by an average of 300%. This indicates that the nanosilica modified asphalt mixture has more possibilities to resist the permanent deformation than the control asphalt mixture at high temperatures. Meanwhile, the resilient modulus of nanosilica modified asphalt mixture is higher than the control asphalt mixture at high temperatures. So, the nanosilica modified asphalt mixture is stiffer than the control asphalt mixture at high temperatures. As indicated above, the nanosilica has a reaction with the asphalt binder, and the nanosilica surface property is changed, which is good for the nanosilica melting and dispersion in the asphalt matrix. More important, the changing of asphalt binders brings the macro performance improvement of nanosilica modified asphalt mixture.

Conclusions

Based on the results of the tests of nano-modified asphalt binder and control asphalt binder PG 58-34, the following conclusions can be drawn:

1. With the addition of nanosilica in the base asphalt binder, the viscosity values of nano-modified asphalt binder decrease slightly. Lower viscosity of the binder indicates that a lower compaction temperature or lower energy consumption of the construction process will be achieved.
2. The complex shear modulus of nanosilica modified asphalt binder generally decreases slightly relative to the control asphalt binder; except that the complex shear modulus of nanosilica modified asphalt binder at 13°C after the PAV aging increases slightly. However, from the rutting and fatigue cracking dissipated work standpoints, nanosilica modified asphalt binder has better high-temperature performance relative to the control asphalt binder before or after the RTFO and PAV aging processes. The addition of nanosilica into the control asphalt improves the recovery ability of asphalt binders.
3. The SEM images show that the microstructure of nanosilica modified asphalt binders changed compared to the control asphalt binder. A good dispersion of nanosilica particles in the asphalt binder matrix is observed.
4. BBR test results show that the low-temperature grade of nanosilica modified asphalt binder is the same as the control asphalt binder, and the properties and stress relaxation capacity of nanosilica modified asphalt binder is the same as the control asphalt binder.
5. With the addition of nanosilica into the control asphalt, the oxidant reactions and aging process of nano-modified asphalt binder are reduced and delayed, as indicated by the ratio changes of chemical bonding.
6. The dynamic modulus of nanosilica modified asphalt mixture increases significantly relative to the control asphalt mixture. The 6% nanosilica modified asphalt mixture has higher dynamic modulus than 4% nanosilica modified asphalt mixture at high temperatures. These indicate that the rutting resistance performance of nanosilica modified asphalt mixture improves.
7. The APA rutting results show the rut depths of nanosilica modified asphalt mixture decrease extremely compared to the control asphalt mixture. This implies that the rutting resistance and antistripping property of nanosilica modified asphalt mixture greatly improve.
8. The flow number and resilient modulus of nanosilica modified asphalt mixture tremendously increase with the addition of nanosilica into the control asphalt mixture. It infers that the additional nanosilica in the asphalt mixture promotes the improvement of rutting resistance.

Therefore, the antiaging performance and fatigue cracking performance of nanosilica modified asphalt binder and mixture are enhanced and the rutting resistance and antistripping property of nanosilica modified asphalt mixture are also enhanced significantly. Meanwhile, the addition of nanosilica into the control asphalt binder does not greatly affect the low-temperature properties of asphalt binders and mixtures. Furthermore, the research team is attempting to fully disperse the nanosilica in the asphalt binder so as to achieve the full potential of the nano-modification, and find out more details about the microstructural changes of nano-modified asphalt binders.

Acknowledgments

The authors would like to thank Su Ting Lau for her help in preparing and testing part of the laboratory work in this research study. The experimental work was completed at Michigan Technological University. Any opinions, findings, and conclusions or

recommendations expressed in this material are those of the authors and do not necessarily reflect the views of any organization.

References

- Al-Hadidy, A., and Yi-qiu, T. (2011). "Effect of Styrene-Butadiene-Styrene on the Properties of Asphalt and Stone-Matrix-Asphalt Mixture." *J. Mater. Civ. Eng.*, 23(4), 504–510.
- Al-Khateeb, G. G., and Al-Akhras, N. M. (2011). "Properties of Portland cement-modified asphalt binder using Superpave tests." *Constr. Build. Mater.*, 25(2), 926–932.
- An, Z., et al. (2012). "Novel peanut-like α -Fe₂O₃ superstructures: Oriented aggregation and Ostwald ripening in a one-pot solvothermal process." *Powder Technol.*, 217(2), 274–280.
- Anurag, K., et al. (2009). "Laboratory investigation of indirect tensile strength using roofing polyester waste fibers in hot mix asphalt." *Constr. Build. Mater.*, 23(5), 2035–2040.
- Arabani, M., et al. (2010). "The effect of waste tire thread mesh on the dynamic behaviour of asphalt mixtures." *Constr. Build. Mater.*, 24(6), 1060–1068.
- Asphalt Institute. (2003). "Superpave performance graded asphalt binder specification and testing." *Superpave Series No. 1(SP-1)* Lexington, KY.
- ASTM. (2008). "Standard test method for determining the flexural creep stiffness of asphalt binder using the bending beam rheometer (BBR)." *D6648*, West Conshohocken, PA.
- ASTM. (2010a). "Standard test method for multiple stress creep and recovery (MSCR) of asphalt binder using a dynamic shear rheometer." *D7405*, West Conshohocken, PA.
- ASTM. (2010b). "Standard test methods for rheological properties of non-Newtonian materials by rotational (Brookfield type) viscometer." *D2196*, West Conshohocken, PA.
- Bahia, H. U., and Anderson, D. A. (1995). "The new proposed rheological properties of asphalt binders: Why are they required and how do they compare to conventional properties." *STP 1241*, Transportation Research Board, West Conshohocken, PA.
- Balazs, A. C., et al. (2006). "Nanoparticle polymer composites: Where two small worlds meet." *Science*, 314(5802), 1107–1110.
- Brown, E. R. (2009). *Hot mix asphalt materials, mixture design and construction*, 3rd Ed., National Asphalt Pavement Association, Lanham, MD.
- Cao, W. (2007). "Study on properties of recycled tire rubber modified asphalt mixtures using dry process." *Constr. Build. Mater.*, 21(5), 1011–1015.
- Chen, Y., et al. (2008). "Natural rubber nanocomposite reinforced with nano silica." *Polym. Eng. Sci.*, 48(9), 1674–1677.
- Chotirat, L., et al. (2007). "On adhesion mechanisms and interfacial strength in acrylonitrile-butadiene-styrene/wood sawdust composites." *Int. J. Adhes. Adhes.*, 27(8), 669–678.
- Cong, P., et al. (2012). "Effects of diatomite on the properties of asphalt binder." *Constr. Build. Mater.*, 30(5), 495–499.
- Cortizo, M. S., et al. (2004). "Effect of the thermal degradation of SBS copolymers during the ageing of modified asphalts." *Polym. Degrad. Stab.*, 86(2), 275–282.
- Ding, P., et al. (2009). "De-agglomeration of hydrophobic and hydrophilic silica nano-powders in a high shear mixer." *Powder Technol.*, 195(3), 221–226.
- Dong, D., et al. (2001). "Thermal degradation of acrylonitrile-butadiene-styrene terpolymer in bean oil." *Polym. Degrad. Stab.*, 73(2), 319–326.
- Goh, S., et al. (2011). "Preliminary dynamic modulus criteria of HMA for field rutting of asphalt pavements: Michigan's experience." *J. Transp. Eng.*, 137(1), 37–45.
- Goh, S., et al. (2011). "Determination of flow number in asphalt mixtures from deformation rate during secondary state." *Transportation Research Record 2210*, Transportation Research Board, Washington, DC, 106–112.
- Goh, S. W., et al. (2007). "Laboratory evaluation and pavement design for warm mix asphalt." *Proc., 2007 Mid-Continent Transportation Research Symp.*, Iowa State Univ., Ames, IA.
- Goh, S. W., and You, Z. (2009). "A simple stepwise method to determine and evaluate the initiation of tertiary flow for asphalt mixtures under dynamic creep test." *Constr. Build. Mater.*, 23(11), 3398–3405.
- Goulias, D. G. (2001). *Design, behavior, and benefits of highway materials using recycled tire rubber. Beneficial use of recycled materials in transportation applications*, Univ. of New Hampshire, Durham, NH, 545–552.
- Greenwood, N. N., and Earnshaw, A. (1998). *Chemistry of the elements*, 2nd Ed., Elsevier, Philadelphia.
- Hansen, K. R., McGennis, R., Prowell, B. D., and Stonex, A. (2000). *Current and future used of non-bituminous components of bituminous paving mixtures*, Transportation Research Board, Washington, DC.
- He, X., and Shi, X. (2008). "Chloride permeability and microstructure of Portland cement mortars incorporating nanomaterials." *Transportation Research Record 2070*, Transportation Research Board, Washington, DC, 13–21.
- Iler, R. K. (1979). *Chemistry of silica—solubility, polymerization, colloid and surface properties and biochemistry*, John Wiley & Sons, New York.
- Khattak, M. J., et al. (2011). "Mechanistic characteristics of asphalt binder and asphalt matrix modified with nano-fibers." *Proc., GeoFrontiers 2011: Advances in Geotechnical Engineering*, ASCE, Reston, VA.
- Khattak, M. J., et al. (2012). "The impact of carbon nano-fiber modification on asphalt binder rheology." *Constr. Build. Mater.*, 30(5), 257–264.
- Kim, J., et al. (2003). "Studies on the thermal stabilization enhancement of ABS: Synergistic effect of triphenyl phosphate nanocomposite, epoxy resin, and silane coupling agent mixtures." *Polym. Degrad. Stab.*, 79(2), 201–207.
- Larsen, D. O., et al. (2009). "Micro-structural and rheological characteristics of SBS-asphalt blends during their manufacturing." *Constr. Build. Mater.*, 23(8), 2769–2774.
- Lazzara, G., and Milioto, S. (2010). "Dispersions of nanosilica in biocompatible copolymers." *Polym. Degrad. Stab.*, 95(4), 610–617.
- Leontaritis, K. J., and Mansoori, G. A. (1988). "Asphaltene deposition: A survey of field experiences and research approaches." *J. Petrol. Sci. Eng.*, 1(3), 229–239.
- Lindberg, H. K., et al. (2008). "Genotoxic effects of fumes from asphalt modified with waste plastic and tall oil pitch." *Mutation Res. Genetic Toxicol. Environ. Mutagen.*, 653(1–2), 82–90.
- Liu, S., et al. (2010). "Analysis and application of relationships between low-temperature rheological performance parameters of asphalt binders." *Constr. Build. Mater.*, 24(4), 471–478.
- Mansoori, G. A. (1997). "Modeling of asphaltene and other heavy organic depositions." *J. Petrol. Sci. Eng.*, 17(1–2), 101–111.
- Mrotzek, M., and Nembach, E. (2008). "Ostwald ripening of precipitates during two successive heat treatments performed at different temperatures." *Acta Mater.*, 56(1), 150–154.
- Odegard, G. M., et al. (2005). "Modeling of the mechanical properties of nanoparticle/polymer composites." *Polymer*, 46(2), 553–562.
- Ouyang, C., et al. (2006). "Improving the aging resistance of asphalt by addition of Zinc dialkyldithiophosphate." *Fuel*, 85(7–8), 1060–1066.
- Peng, Z., et al. (2007). "Self-assembled natural rubber/silica nanocomposites: Its preparation and characterization." *Compos. Sci. Technol.*, 67(15–16), 3130–3139.
- Peters, S., et al. (2010). "Nanocellulose and microcellulose fibers for concrete." *Transportation Research Record 2142*, Transportation Research Board, Washington, DC, 25–28.
- Probst, C., et al. (2007). "Imaging of carbon nanotubes with tin-palladium particles using STEM detector in a FE-SEM." *Micron*, 38(4), 402–408.
- Putman, B. J., and Amirkhanian, S. N. (2004). "Utilization of waste fibers in stone matrix asphalt mixtures." *Resour. Conserv. Recycl.*, 42(3), 265–274.
- Shen, J., et al. (2009). "Influence of surface area and size of crumb rubber on high temperature properties of crumb rubber modified binders." *Constr. Build. Mater.*, 23(1), 304–310.
- Shi, X., et al. (2012). "Exploring the interactions of chloride deicer solutions with nanomodified and micromodified asphalt mixtures using artificial neural networks." *J. Mater. Civ. Eng.*, 24(7), 805–815.

- Shiman, L., et al. (2011). "Effects of nanocomposites on the high temperature rheological properties of a PG58 asphalt-binder." *Proc. GeoHuman 2011 Int. Conf.*, ASCE, Reston, VA.
- Sugimoto, T. (2000). *Fine particles: Synthesis, characterization, and mechanisms of growth*, Marcel Dekker, New York.
- Sun, Y., et al. (2008). "Preparation and properties of natural rubber nanocomposites with solid-state organomodified montmorillonite." *J. Appl. Polym. Sci.*, 107(5), 2786–2792.
- Wiberg, E., et al. (2001). *Inorganic chemistry*. San Diego; Berlin; New York, Academic Press; De Gruyter.
- Witczak, M. W. (2007). "Specification criteria for simple performance tests for rutting." *NCHRP Rep. 580*, Transportation Research Board, Washington, DC.
- Witczak, M. W., Kaloush, K., Pellinen, T., El-basyouny, M., and Von Quintus, H. (2002). "Simple performance test for superpave mix design." *NCHRP Rep. 465*, Transportation Research Board, Washington, DC.
- Xiao, F., et al. (2009). "Influences of crumb rubber size and type on reclaimed asphalt pavement (RAP) mixtures." *Constr. Build. Mater.*, 23(2), 1028–1034.
- Xiao, F., et al. (2011). "Influence of carbon nanoparticles on the rheological characteristics of short-term aged asphalt binders." *J. Mater. Civ. Eng.*, 23(4), 423–431.
- Xu, T., and Huang, X. (2010a). "Study on combustion mechanism of asphalt binder by using TG-FTIR technique." *Fuel*, 89(9), 2185–2190.
- Xu, T., and Huang, X. (2010b). "A TG-FTIR investigation into smoke suppression mechanism of magnesium hydroxide in asphalt combustion process." *J. Anal. Appl. Pyrol.*, 87(2), 217–223.
- Yao, H., et al. (2012). "Performance of asphalt binder blended with non-modified and polymer-modified nanoclay." *Constr. Build. Mater.*, 35(10), 159–170.
- Yildirim, Y. (2007). "Polymer modified asphalt binders." *Constr. Build. Mater.*, 21(1), 66–72.
- You, Z., et al. (2011). "Nanoclay-modified asphalt materials: Preparation and characterization." *Constr. Build. Mater.*, 25(2), 1072–1078.
- You, Z., Goh, S. W., and Williams, R. C. (2009). "Development of specification for the Superpave simple performance tests (SPT)." *Final Rep. RC-1532*, Michigan Department of Transportation, Lansing, MI, 220.
- Yu, J., et al. (2007a). "Effect of montmorillonite on properties of styrene-butadiene-styrene copolymer modified bitumen." *Polym. Eng. Sci.*, 47(9), 1289–1295.
- Yu, J., et al. (2007b). "Preparation and properties of montmorillonite modified asphalts." *Mater. Sci. Eng. A*, 447(1–2), 233–238.
- Yu, J.-Y., et al. (2009). "Effect of organo-montmorillonite on aging properties of asphalt." *Constr. Build. Mater.*, 23(7), 2636–2640.
- Zhang, B., et al. (2009). "The effect of styrene-butadiene-rubber/montmorillonite modification on the characteristics and properties of asphalt." *Constr. Build. Mater.*, 23(10), 3112–3117.
- Zhang, F., et al. (2011). "Effects of thermal oxidative ageing on dynamic viscosity, TG/DTG, DTA and FTIR of SBS- and SBS/sulfur-modified asphalts." *Constr. Build. Mater.*, 25(1), 129–137.
- Zhang, F., and Yu, J. (2010). "The research for high-performance SBR compound modified asphalt." *Constr. Build. Mater.*, 24(3), 410–418.
- Zhang, H., et al. (2005). "Study on flammability of montmorillonite/styrene-butadiene rubber (SBR) nanocomposites." *J. Appl. Polym. Sci.*, 97(3), 844–849.